ingegneria sismica
International Journal of Earthquake Engineering
Anno XLIII - Num. 1 - 2026

Simulation of Urban Flooding Dynamics Based on LSTM-CNN Hybrid Modeling

Kang Yang[1], *Jiahao Fu*[2,3,*] *and Huizhen Fan*[1]

[1] School of Geography and Tourism, Luoyang Normal University, Luoyang, 471934, Henan China
[2] Zhejiang Economic Information Center, Hangzhou 310006, Zhejiang China
[3] Zhejiang Economic Information Development Co., Ltd., Hangzhou 310006, Zhejiang China

SUMMARY: *In this paper, a hybrid LSTM-CNN model is constructed to realize the dynamic simulation of urban flooding, which is realized by multi-layer perception of neurocognitive machine and feature recognition through convolutional computation. The model network identifies the site rain feature variables that may produce dangerous waterlogged areas by learning local spatial features for identifying the magnitude of surface generated runoff under different rainfall events and their impact on the city. The common urban flooding scenarios caused by river and heavy rainfall and other disaster-causing factors are simulated as a source of urban flooding data by fully considering the hydrological characteristics of the city and following the principles of hydrology-hydrodynamics. The normalization method was adopted to pre-process the data, the entropy method was used to determine the weights of the indicators, the effective threshold of water depth was defined, and the mean absolute error (MAE), root mean square error (RMSE), and Nash efficiency coefficient (NSE) were selected as the evaluation indicators. Taking Henan Province as the study area for empirical analysis, the LSTM-CNN hybrid model achieves a forecasting accuracy of 92.5% in the flood peak flow and peak present time, and realizes the spatial-temporal evolution analysis of the mildly, moderately, and severely affected populations in the dynamic simulation of the population risk in the whole process of urban rainstorms and floods. Based on the LSTM-CNN hybrid model can sense urban flooding in real time and provide an effective tool for risk assessment and emergency management.*

KEYWORDS: *hybrid LSTM-CNN model; convolutional computation; urban flooding; dynamic simulation; hydrological-hydrodynamic*

1 Introduction

With the intensification of global climate change and urbanization, heavy rainfall-flood disasters are characterized by strong suddenness and short foresight period [1]. The complexity and uncertainty of its spatial and temporal changes are becoming more and more prominent, and the simulation and early warning of storm-flood disaster has become a hot frontier of current academic research. Urban storm flood simulation is one of the key technologies for urban flood prevention and mitigation, and the construction of a specific urban rainfall and flood model based on the production and sink characteristics of urban areas can provide

*jh.fu@outlook.com
https://doi.org/10.65102/is2026020
Published: 30 April, 2026

scientific and reliable technical support for the solution of urban flood prevention and drainage, rainfall utilization, surface pollution research, rainfall and flood regulation and storage of urban hydrological problems, so as to reduce the losses, safeguard the safety of people's lives and properties, improve the urban water environment, and achieve sustainable and healthy urban development [2]. Flooding is one of the most common and serious types of natural disasters in China, and the number of deaths, the number of affected population and economic losses caused by floods rank first in the ranking of natural disaster events [3]. In recent years, the increasing level of urbanization, the increase of high-rise buildings, the irrational urban spatial layout, and the mismatch of infrastructures have made China's urban heavy rainfall and flooding disasters characterized by complexity, diversity, chaining, and amplification [4].

Li, G. et al. conducted reproduction and simulation of flood disaster site, constructed a coupled urban storm-flood model and conducted experiments. The results showed that the ratio of rainfall and urban storm inundation was 0.8776 and the ratio of inundation time was 0.8241, and this study is important for urban flood prevention and mitigation [5]. Shi, Y. et al. Disaster prevention and mitigation programs for flood hazards based on risk assessment, constructed a flood disaster risk indicators, risk factors, adding precipitation factors to the flood assessment. Xiamen, as an example, Xiamen in in large-scale typhoon precipitation impacts of the coefficient of variation, high risk, and should be set up to prevent flooding new priority areas, for which a new response program is proposed, and the study of the extension of flood risk assessment [6]. Moon, H. et al. explored the potential of machine learning approach Random Forest as an alternative model for urban flood prediction by performing training on topography and environment, the results showed that the agent model has a significantly shorter runtime than the physical model, and that machine learning with high resolution and high fidelity can significantly enhance urban flood management decisions [7]. Shao, Y. et al. study introduced a novel deep learning model called CRU-Net equipped with an attention mechanism to predict flooding depth in urban terrain based on spatio-temporal rainfall patterns. The deep learning model was developed through eight urban waterlogged terrain parameters and rainfall data model data, and the model can skillfully interpret the spatio-temporal characteristics of rainfall and predict the flooding depths with more than 80% accuracy, demonstrating its high efficiency [8]. Xu, C. et al. investigated the performance of deep learning techniques and hydrological modeling, constructed a distributed hydrological model based on remote sensing data, and the model could be applied to the Western Basin with satisfactory results. The results show that deep learning basin-scale water environment management and enhancement of hydrological disaster warning are meaningful [9]. Li, X. et al. discussed the impacts of flood disasters on Zhengzhou, Henan Province, which increased severe losses to city residents, and studied the flood emergency response capacity. The model was evaluated by a combination of entropy weighting method and coefficient of variation method [10].

A large number of existing studies are based on the theoretical assumption of a stable environment, and the use of static data-driven reactive simulation methods has led to the problem of “data lag, analysis lag, and decision-making lag”, which is becoming increasingly prominent. Aiming at the complexity and uncertainty of the spatial and temporal changes of the rainstorm-flood process, this paper proposes a hydrological change-driven active simulation method, establishes a dynamic coupling mechanism between the dynamic hydrological observation data and the simulation process, and portrays the spatial and temporal consistency of the relationship between hydrological observation information and the flood process, which further enhances the real-time sensing, cognition, and quantitative analysis capability of the spatial and temporal changes of the rainstorm-flood process. In this paper, a hybrid LSTM-CNN model is created, and the convolutional neural network is based on the multi-layer perception of the neurocognitive machine, which is combined with the error propagation

algorithm to realize the recognition of features. The created hybrid model of LSTM-CNN is used to simulate flooding scenarios in cities caused by river, heavy rain and other disaster-causing factors, and the recognition results are used as the disaster elements and data sources. By normalizing the positive indicators, calculating the weights by entropy method, setting the depth of water accumulation and 95% confidence interval, the mean absolute error (MAE), root mean square error (RMSE) and Nash efficiency coefficient (NSE) are used as the assessment indicators. The feasibility of the hybrid LSTM-CNN model in the dynamic simulation of urban flooding is verified in Henan Province as an example.

2 Hybrid model based on LSTM-CNN

2.1 LSTM-CNN modeling

2.1.1 Working mechanism

Convolutional Neural Network (CNN) is essentially a multilayer perception based on a neurocognitive machine and the working mechanism of neurocognition is shown in Figure 1. The neurocognitive machine takes the input feature variables and extracts them locally, and then enters the hierarchical stepwise connected feature planes for processing, going through this process repeatedly [11]. The local features extracted at the bottom layer will gradually become global features, and the recognition of the features is achieved by introducing an error propagation algorithm [12].

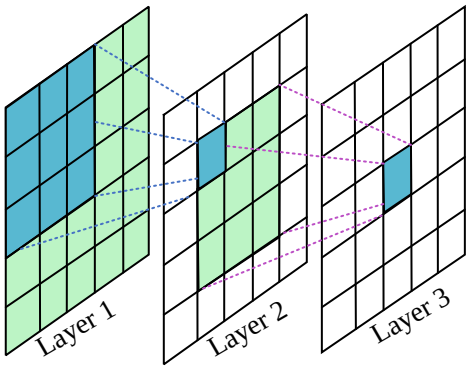

Figure 1: Working mechanism of neurocognition

The typical structure of LSTM-CNN network evolved from the neurocognitive machine, Figure 2 shows the structure of LSTM-CNN network. Recognition of features is achieved by connecting the convolutional layer pooling layer, activation layer, fully connected layer and some auxiliary layers. The convolutional layer learns local patterns through weight sharing and convolutional computation, and the pooling layer plays the effect of downsampling and expanding the sense field of view through downsampling, and this network has been widely used in dynamic simulation research [13, 14].

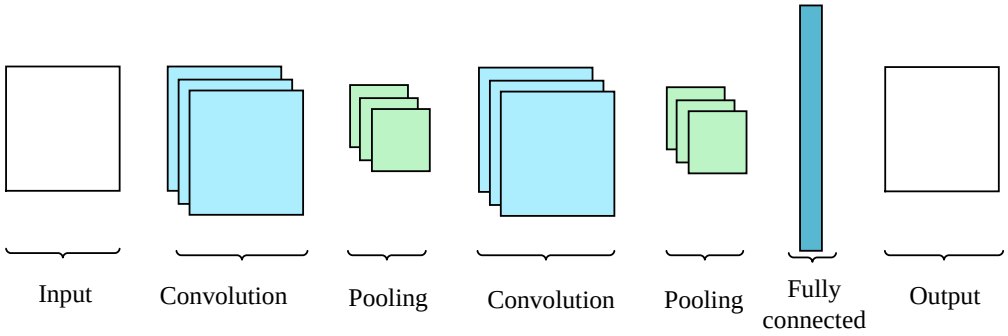

Figure 2: LSTM-CNN network structure

2.1.2 Convolutional computation

The convolutional layer is the core of the CNN network structure, which extracts and computes the features based on the size of its own field of view, and undertakes the most important task of feature extraction and transfer in the whole network [15, 16]. The formula for this layer is shown below:

$$Y^1(m,n) = x^k(m,n) * H^{KI}(m,n) = \sum_{k=0}^{k-1}\sum_{i-0}^{I-1}\sum_{j=0}^{J-1} X^k(m+i,n+j)H^{KI}(i,j) \tag{1}$$

where * represents the convolutional computation, I and J denote the dimensions of the convolutional kernel, K and L represent the number of channels in the input and output layers, respectively, X^K and Y^1 represent the two-dimensional feature matrices of the K th input channel and the 7th output channel, respectively, and H^{KI} represents the convolution kernel at this point.

2.1.3 Basic structure of the forecasting model

Compared to ordinary fully connected neural networks, convolutional neural networks have two distinctive features. One is sparse interaction, for each layer of the convolutional layer, the scale of the convolutional kernel is much smaller than the dimension of the input data. This allows the neuron nodes in each layer to respond only to neurons within the local region of the previous layer, providing stronger feature extraction capabilities. Secondly, parameter sharing, in convolutional neural networks, the convolutional kernels in the same layer share the same weights, and the weights in the convolutional kernel will act on a specific location in each local input, which makes the number of parameters significantly reduced. According to the idea of parameter sharing, the network only needs to learn a set of parameter sets without optimizing each parameter for each position, which greatly reduces the storage requirements of the model.

In the problem of predicting urban flooding, since the flow and pooling of water will be affected by the surrounding terrain environment, the sparse interaction feature makes the convolutional neural network more suitable for learning and recognizing these flood-prone vulnerable points. And the feature of parameter sharing makes the convolutional layer of the convolutional neural network with translational isotropy, so that the model is able to recognize any flood-prone locations, no matter where they are located. The urban flood prediction infrastructure is shown in Fig. 3, where the network learns local spatial features and then combines these local features to form more complex and abstract features for identifying the parts of the city that may produce hazardous waterlogged areas, while the rainfall feature variables are used to identify the magnitude of runoff generated from the surface under different

rainfall events and their impact on the city [17]. Finally, all features are combined and mapped to their relationship with water depth, and the water depth magnitude for each grid is output to obtain the inundation inundation map of the study area [18].

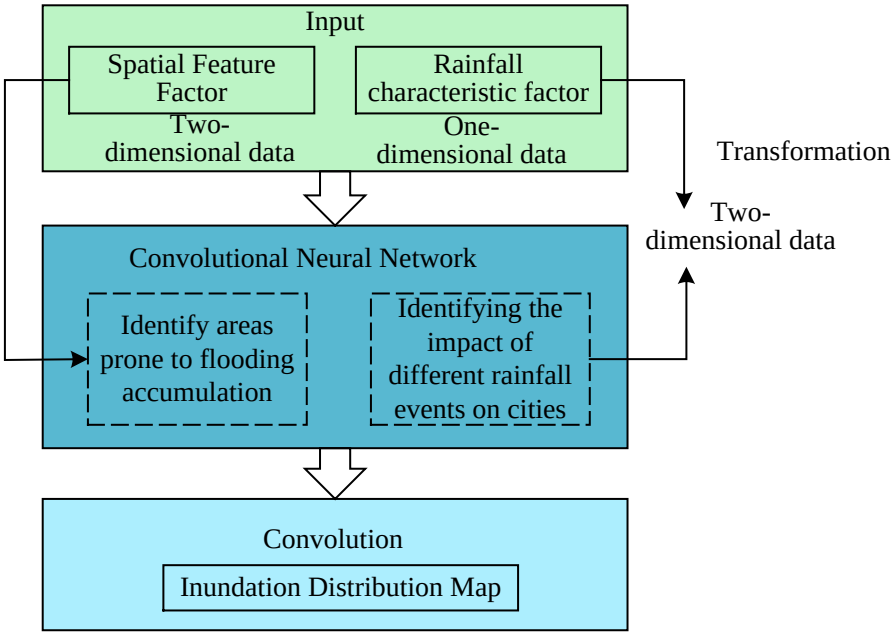

Figure 3: Urban flood prediction infrastructure

2.2 Flood time series dataset generation

Urban flood simulation is an important method to obtain urban flood information, through flood simulation can be obtained under different urban flood disaster scenarios of the risk characteristics and continuous disaster process, so urban flood simulation is increasingly used in urban flood risk and vulnerability research [19]. On the other hand, compared with natural watershed flood simulation, urban areas may have more complex topography and subsurface characteristics leading to more complex flood drainage processes, which requires more elemental characteristics to be considered in the urban flood simulation process in order to realize the refined simulation of urban flood hazards. In this paper, from the urban hydrological characteristics, following the principle of hydrology-hydrodynamics, the hybrid model of LSTM-CNN creates an urban coupled flooding model, which is used to simulate common urban flooding scenarios caused by rivers, heavy rainfall and other disaster-causing factors, and serves as an important source of disaster elements and data in the quantitative study of urban flood vulnerability [20, 21].

The urban flood disaster scenarios are shown in Figure 4, and the disaster-causing factors and urban drainage process are important objects in urban flood simulation. Affected by the geographic environment, hydrometeorological elements, urban areas may be subject to different types of flooding disasters, such as river flooding, heavy rainfall, storm surges, etc. may lead to the occurrence of urban flooding. When rainfall or river water enters the urban drainage system, the development process determines whether flooding occurs or not.

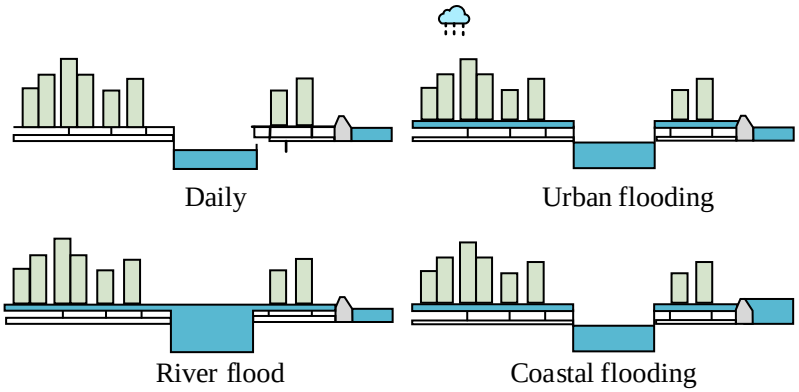

Figure 4: Urban flooding scenario

When rainfall, river floods and other disaster-causing factors appear, its drainage process after entering the urban environment is the key object of urban flood simulation. Drainage system is an important infrastructure in the urban environment, for large cities or infrastructure more perfect urban areas, its drainage system can be subdivided into sewage drainage system and stormwater drainage system, the drainage system in this paper mainly refers to the urban flood prevention and flood control closely related to the stormwater drainage system. Secondly, there is a big difference between the urban drainage process and the natural watershed catchment process, the drainage of the natural area is mainly through the surface of the catchment into and through all levels of the river network discharge, while the city not only has a variety of surface types, rivers, drainage canals and so on. At the same time, the region is also dotted with different levels of urban drainage pipe network and a variety of other artificial drainage facilities, such as pumping stations, gates, etc., these urban drainage facilities and rivers, etc. together constitute the urban drainage system. Can be in the city in the flood disaster, the excess water in the city in a timely manner, these complex drainage processes need to be realized in the urban flood simulation.

2.3 Determination of indicator weights

2.3.1 Data pre-processing

As the urban flood vulnerability indicators have different units of measurement, the indicator values in the range of large differences, the need to use a dimensionless method to ensure uniform standardization among the indicators to reduce the impact of the indicator order of magnitude on the indicators, so the normalization method is taken to do the following pre-processing of the indicator data. The normalization formula for positive indicators is as follows:

$$x_{ij}^{'} = \frac{x_{ij} - \min\left\{x_{ij}, \cdots, x_{mj}\right\}}{\max\left\{x_{ij}, \cdots, x_{mj}\right\} - \min\left\{x_{1j}. \cdots, x_{mj}\right\}} \tag{2}$$

The normalized formula for the negative indicator is as follows:

$$x_{ij}^{'} = \frac{\max\left\{x_{ij}, \cdots, x_{mj}\right\} - x_{ij}}{\max\left\{x_{ij}, \cdots, x_{mj}\right\} - \min\left\{x_{1j}. \cdots, x_{mj}\right\}} \tag{3}$$

where: x denotes the value of the j th indicator in the i th city, $i = 1, 2, \cdots, m; j = 1, 2, \cdots, n$. The $x_{ij}^{'}$ is the normalized value, and for convenience, the normalized data in the following

calculations are still recorded as x_{ij} .

2.3.2 Entropy method to calculate weights

In the entropy method of determining indicator weights, the formula for calculating the proportion of the i th city under the j th indicator to that indicator is as follows:

$$P_{ij} = \frac{x_{ij}}{\sum_{i=1}^{m} x_{ij}} \tag{4}$$

The formula for calculating the entropy value of the j th indicator is as follows:

$$e_j = -k\sum_{i=1}^{m} P_{ij} 1n(p_{ij}) \tag{5}$$

The formula for calculating the information entropy redundancy of the j th metric is as follows:

$$d_j = 1 - e \tag{6}$$

The formula for calculating the weights of the indicators is as follows:

$$w_i = \frac{d_j}{\sum_{j=1}^{n} d_j} \tag{7}$$

Indicators with positive attributes indicate that the greater the value of the indicator, the higher the vulnerability to urban flooding. Indicators with negative attributes indicate that the larger the value of the indicator, the lower the vulnerability to urban flooding.

2.3.3 Target data sets

Considering the areas with shallow flood depths, neither damage to public or private property nor the normal operation of the city will be affected, but rather the predictive ability of the model. Therefore the results for the water depth should be corrected, and the traffic is more significantly affected by the water depth when the water depth reaches 5 cm. Therefore in this study all water depth parts less than 0.05m are truncated as shown in equation (8):

$$Y = \begin{cases} 0 x \le 0.05 \\ x x \rangle 0.05 \end{cases} \tag{8}$$

where x represents the water depth obtained from the simulation. y represents the modified depth of standing water input into the model, as the output variable 0.05m is the value to determine whether the water depth is too shallow.

2.3.4 Training process

The mean and standard deviation are obtained for the output approximate posterior distribution, where the mean is used as the predicted value of water depth in this paper, and the standard

deviation is used to quantify the uncertainty as well as to construct confidence intervals to get the interval prediction value of water depth in the study area. If a 95% confidence interval is constructed, the prediction of water depth with uncertainty can be obtained, and the formula for calculating the 95% confidence interval is shown below:

$$CI = \left[\mu - 1.96 \times \sigma, \mu + 1.96 \times \sigma\right] \tag{9}$$

The construction and training process of the model proposed in this paper are based on the implementation of Torch 1.1 framework in Python programming language, and in order to accelerate the computation speed, the training process is accelerated by using a NVIDIA RTX A4000 GPU with 16gb of memory throughout the whole process.

2.3.5 Model Validation and Accuracy Evaluation Metrics

In this paper, Mean Absolute Error (MAE), Root Mean Square Error (RMSE) and Nash Efficiency Coefficient (NSE) are selected as evaluation metrics used to assess the ability of the LSTN-CNN model to directly compare the simulation results with those of the other models and quantify the prediction errors.

The mean absolute error (MAE) is the average of the absolute errors, reflecting the average absolute deviation between the model-predicted bathymetry values and the results obtained from the hydrodynamic model. Its calculation formula is shown below:

$$MAE = \frac{\sum_{i=1}^{N} \left| y_{pre} - y_{sim} \right|}{N} \tag{10}$$

where y_{pre} and y_{sim} represent the water depth values computed with the deep learning model and hydrodynamic model, respectively, and m, N is the sample capacity. The smaller the MAE value indicates that the error between the two is smaller, and the results obtained by the model prediction have a higher accuracy.

Root Mean Square Error (RMSE) is a measure of the overall error between the model prediction data and the observed data, as is MAE, with the difference that RMSE squares the error and magnifies the gap between larger errors, and is therefore more sensitive compared to MAE. Its calculation formula is shown below:

$$RMSE = \sqrt{\frac{\sum_{i=1}^{N} (y_{pre} - y_{sim})^2}{N}} \tag{11}$$

RMSE is usually greater than 0. When its value tends to 0, it proves that the LSTN-CNN model has good stability in simulating the inundation depth of urban flooding.NSE is a dimensionless goodness-of-fit measure, and its formula is shown below:

$$NSE = 1 - \frac{\sum_{i=1}^{N} (y_{pre} - y_{sim})^2}{\sum_{i=1}^{N} (\bar{y}_{sim} - y_{sim})^2} \tag{12}$$

In the formula, $\bar{y}_{sim}$ represents the average value of water depth calculated by the hydrodynamic model. The NSE value varies between 0 and 1. The larger the value, the more ideal the fit between the predicted data and the observed data. This indicator is widely used in the evaluation of hydrological models. An NSE value greater than 0.9 is considered "very

satisfactory", values between 0.8 and 0.9 are "quite good", and values less than 0.8 are "unsatisfactory".

2.4 Overview of the study area

Based on the quantitative model of urban flood vulnerability constructed in this paper, Henan Province, for example, is located in the middle and lower reaches of the Yellow River in the North China Plain of China, between longitude 110°21'~116°39'E and latitude 31°23'~36°22'N. The province is connected to Shandong and Anhui in the east, Shaanxi in the west, Hebei and Shanxi in the north, and Hubei in the south. The topography of Henan Province is low in the east and high in the west, and at the same time, it spans four major river basins, namely the Yellow River, Huaihe River, Haihe River, and Yangtze River, with a rich variety of watersheds totaling more than 1,500 main rivers. Because the topography of Henan Province is mainly plains and basins, and has rich watershed resources, it often faces natural disasters such as floods and urban waterlogging. The experimental data mainly consists of basic geographic information data, socio-economic data and historical disaster data. The basic geographic information data, including water systems, roads, underground drainage networks, digital elevation models, and organizational location points, are obtained from the Geographic Information Center (GIC).

3 Analysis of hybrid model dynamic simulation results

3.1 Model performance comparison results

In this paper, the relative error between the calculated data and the actual data, the Nash coefficient (NSE), is used to evaluate the LSTM-CNN forecasting results constructed in this paper. Based on the structure of the trained convolutional neural network model, first input urban flooding for model simulation calculation, the model results will be inverse normalized output, model input and output effects. Table 1 Error analysis of model test results, and then all the remaining test sample data are input into the model for model testing.

According to the sample values and fitted values of the test samples, the relative error of flood peak is 9.38% with single-field flooding as the object of analysis, and the simulation effect is good. Taking the field flood as the object of analysis, the error analysis of the flood peak flow and peak present time, from the analysis results, the maximum value of the relative error of the flood peak is 6. From the model simulation results, it can be seen that the model simulation effect on the flood with larger magnitude is better than that of the flood with smaller magnitude, and in the process of the model simulation of field flood, the simulation of the rising effect of the flood is better than the effect of the receding water. Analyzing the reasons for the above results, first of all, floods with larger magnitude have higher rainfall intensity, and the input data of the model are more accurate, which makes the simulation results better. The flood recession process is affected by multiple factors, and the model developed in this paper considers the factors more comprehensively, which leads to the simulation of the flood rise effect is better than the recession effect.

Table 1: Error analysis of model test results

Field	Sample Flood Flows	Fitted Flood Flows	Peak-Present Time Difference	Relative Error/percentage
1	1234.12	1062.6578	0	9.24
2	925.64	812.51	0	9.64
3	659.83	687.91	6	2.93
4	1256	1161.12	6	6.10
5	784.83	784.21	0	6.73
6	1027.41	1124.62	0	14.95
7	391.22	457.12	0	19.32
8	1081.14	1245.67	0	5.1
9	1235.21	1234.61	0	4.92

Based on the hydrological data of the study area, the traditional API model was used to compare with the hybrid LSTM-CNN model. The historical hydrological data of the study area were selected and the 6h integrated unit line was used for flood forecasting, and the model forecasting results are shown in Table 2. The flood peak flow and peak present time were used as evaluation factors to analyze the forecasting results, and the accuracy of flood forecasting using the model was 92.5% after comparative analysis.

Table 2: Comparison of model forecast results

Model	Flood peak wander error/%	Peak present time error/h	Forecast accuracy/%
Traditional API model	4.5	5.2	78.1
Hybrid LSTM-CNN model	1.1	0.7	92.5

The results of the model test are shown in Fig. 5, where the difference between the forecast flow and the measured flow error is small within the five time points. For example, at time point 5, the forecast flow is 145$m^3 \cdot s^{-1}$ and the measured flow is 129 $m^3 \cdot s^{-1}$, with a difference of 11.03%. At time point 1, the predicted and measured flows are close to coinciding.

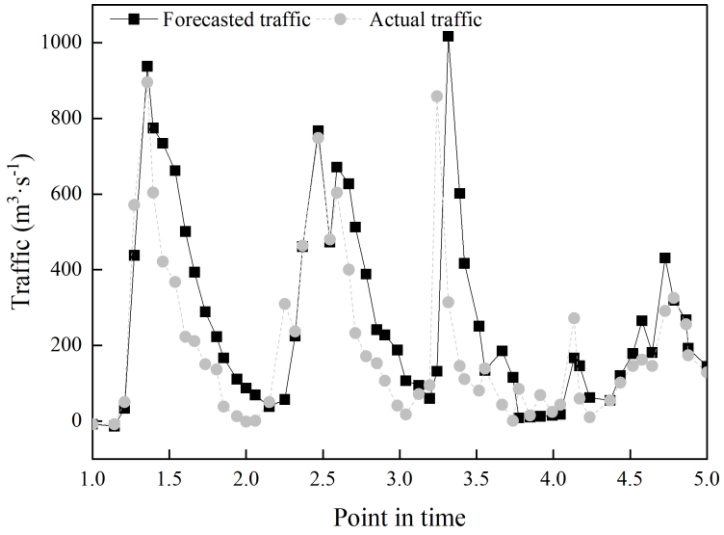

Figure 5: Model test results

3.2 Simulation of population risk dynamics throughout the flooding process

Taking 2h as the sampling interval, the artificial risk dynamic simulation results of the affected population, mildly affected population, moderately affected population and severely affected population in Henan region during the whole process of heavy rainfall and flooding are shown in Figure 6. Among them, the affected population is the sum of the number of mildly affected population, moderately affected population and severely affected population. It can be seen that at 7h, the total affected population is the largest, reaching 527 people, and the simulation results show that the constructed model is able to dynamically analyze the population risk of three different affected states, namely, mild, moderate and severe, during the whole process of the rainstorm. The experimental results prove that the LSTM-CNN hybrid model can dynamically assess the dynamic changes of population risk in the whole process of heavy rainfall and flooding, and can solve the systematic complexity and dynamic changes of population risk in the process of heavy rainfall and flooding, which helps to further study and analyze the complex systems of heavy rainfall and flooding.

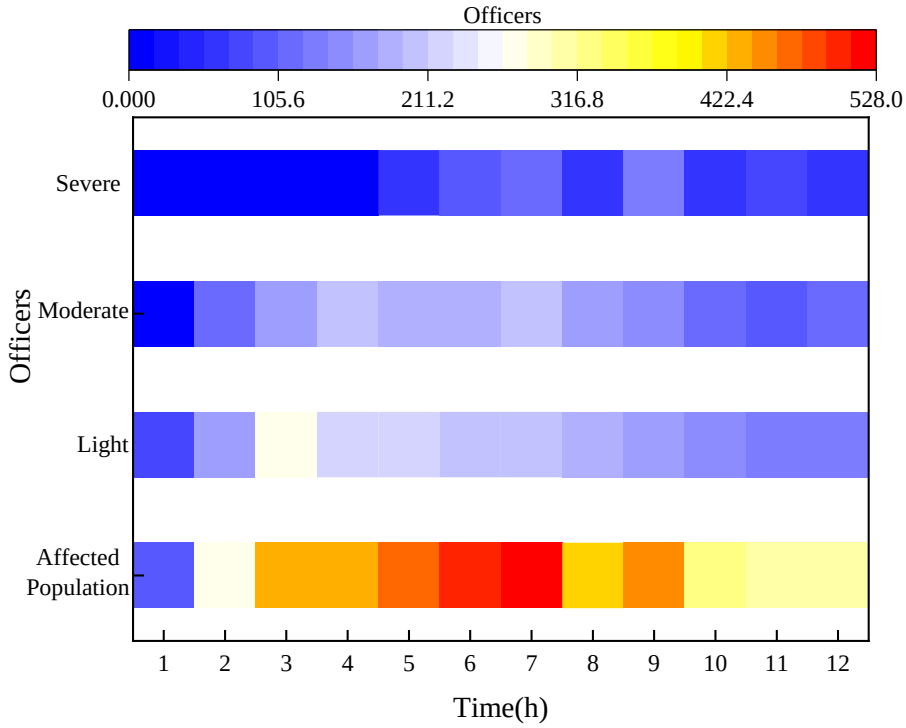

Figure 6: Artificial risk dynamic simulation results

The simulation process of storm flood simulation is divided into three phases, namely, pre-simulation, mid-simulation and post-simulation. The pre-simulation period corresponds to the 4h from the beginning of rainfall to the peak of rainfall, the mid-simulation period corresponds to the 4h after the peak of rainfall, and the post-simulation period corresponds to the 4h from the cessation of rainfall to the end of the simulation. Four different degrees of the population, the affected population, the mildly affected population, the moderately affected population, and the severely affected population, were statistically analyzed in terms of the proportion of the total population. The results of the statistics of the affected population during the whole process of storm flooding are shown in Fig. 7, for the population at mild risk, it began to appear in the 1h of the pre-storm flooding period, peaked in the 1h, and continued to the late stage of the storm, with its peak appearing in the 1h of the storm, accounting for 95% of the total population.

For the population at moderate risk, it shows a gradual increase in the 6h of the simulation, and a gradual decrease in the 9h and 10h of the simulation, with the peak occurring in the 4h of the rainstorm, accounting for 48% of the total population. In contrast, the population at severe risk begins to appear after 4h of the simulation and peaks at 9h in the middle of the storm, accounting for 30% of the total population, and then gradually decreases. For any statistical time point in the simulation, the population at mild risk is larger than the population at moderate risk or the population at severe risk, while the population at moderate risk is larger than the population at severe risk.

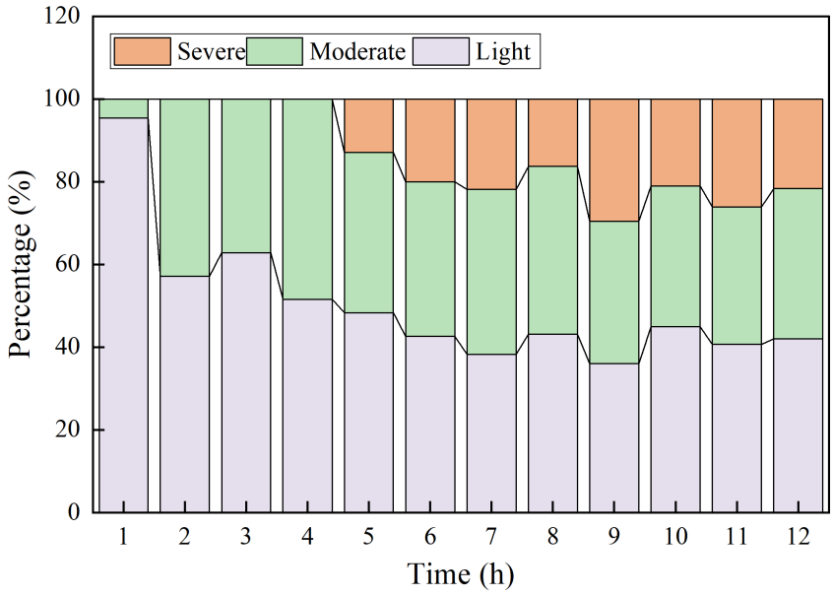

Figure 7: Results of the population affected by the whole process of rainstorms and floods

4 Conclusion

In this study, by constructing and validating the LSTM-CNN hybrid model, the high-precision dynamic simulation and risk assessment of the urban storm-flooding process are realized, and the empirical analysis is based on Henan Province as an example, and the main conclusions are as follows:

(1) The results of model performance comparison show that the integrated accuracy of flood forecasting of LSTM-CNN hybrid model reaches 92.5%, the maximum value of relative error of flood peak is 6, and the relative error of flood peak is 9.38%. The model established in this paper is more comprehensive in its consideration of factors and achieves better simulation results.

(2) The results of the dynamic simulation of population risk in the whole process of flooding show that the total population affected by the flood reaches up to 527 people at the simulation time of 7h. The mildly affected population starts to appear at 1h in the pre-storm flooding period, reaches the peak at 1h, and continues to the late stage of the storm, and its peak appears at 1h of the storm, accounting for 95% of the total population. The dynamic change characteristics of population risk in the pre-flood, mid-flood and post-flood periods are revealed, which proves the ability of LSTM-CNN model to deal with the dynamics of complex systems.

The LSTM-CNN hybrid model constructed in this study provides an effective solution for the refined simulation, real-time early warning and risk dynamic assessment of urban flooding, and it is necessary to further integrate more factors affecting the receding process to realize the

whole process simulation of urban flooding in future research work.

References

[1] Marengo, J. A., Seluchi, M. E., Cunha, A. P., Cuartas, L. A., Goncalves, D., Sperling, V. B., ... & Moraes, O. L. (2023). Heavy rainfall associated with floods in southeastern Brazil in November–December 2021. *Natural Hazards*, 116(3), 3617-3644.

[2] Sun, Y., Liu, C., Du, X., Yang, F., Yao, Y., Soomro, S. E. H., & Hu, C. (2022). Urban storm flood simulation using improved SWMM based on K-means clustering of parameter samples. *Journal of Flood Risk Management*, 15(4), e12826.

[3] Lan, T., Hu, Y., Cheng, L., Chen, L., Guan, X., Yang, Y., ... & Pan, J. (2022). Floods and diarrheal morbidity: Evidence on the relationship, effect modifiers, and attributable risk from Sichuan Province, China. *Journal of global health*, 12, 11007.

[4] Chan, F. K. S., Yang, L. E., Scheffran, J., Mitchell, G., Adekola, O., Griffiths, J., ... & McDonald, A. (2021). Urban flood risks and emerging challenges in a Chinese delta: The case of the Pearl River Delta. *Environmental Science & Policy*, 122, 101-115.

[5] Li, G., Zhao, H., Liu, C., Wang, J., & Yang, F. (2022). City flood disaster scenario simulation based on 1D–2D coupled rain–flood model. *Water*, 14(21), 3548.

[6] Shi, Y., Zhai, G., Zhou, S., Lu, Y., Chen, W., & Deng, J. (2019). How can cities respond to flood disaster risks under multi-scenario simulation? A case study of Xiamen, China. *International journal of environmental research and public health*, 16(4), 618

[7] Moon, H., Yoon, S., & Moon, Y. (2023). Urban flood forecasting using a hybrid modeling approach based on a deep learning technique. *Journal of Hydroinformatics*, 25(2), 593-610.

[8] Shao, Y., Chen, J., Zhang, T., Yu, T., & Chu, S. (2024). Advancing rapid urban flood prediction: a spatiotemporal deep learning approach with uneven rainfall and attention mechanism. *Journal of Hydroinformatics*, 26(6), 1409-1424.

[9] Xu, C., Wang, Y., Fu, H., & Yang, J. (2022). Comprehensive analysis for long-term hydrological simulation by deep learning techniques and remote sensing. *Frontiers in earth science*, 10, 875145.

[10] Li, X., Li, M., Cui, K., Lu, T., Xie, Y., & Liu, D. (2022). Evaluation of comprehensive emergency capacity to urban flood disaster: An example from Zhengzhou city in henan province, China. *Sustainability*, 14(21), 13710.

[11] Munawar, H. S., Ullah, F., Qayyum, S., Khan, S. I., & Mojtahedi, M. (2021). UAVs in disaster management: Application of integrated aerial imagery and convolutional neural network for flood detection. *Sustainability*, 13(14), 7547.

[12] Guo, Z., Leitao, J. P., Simões, N. E., & Moosavi, V. (2021). Data-driven flood emulation: Speeding up urban flood predictions by deep convolutional neural networks. *Journal of Flood Risk Management*, 14(1), e12684.

[13] Lazin, R., Shen, X., & Anagnostou, E. (2021). Estimation of flood-damaged cropland area using a convolutional neural network. *Environmental Research Letters*, 16(5), 054011.

[14] Tsangaratos, P., Ilia, I., Chrysafi, A. A., Matiatos, I., Chen, W., & Hong, H. (2023). Applying a 1D convolutional neural network in flood susceptibility assessments—The case of the Island of Euboea, Greece. *Remote Sensing*, 15(14), 3471.

[15] Panahi, M., Khosravi, K., Rezaie, F., Ferreira, C. S., Destouni, G., & Kalantari, Z. (2023). A country wide evaluation of Sweden's spatial flood modeling with optimized convolutional neural network algorithms. *Earth's Future*, 11(11), e2023EF003749.

[16] Chen, C., Hui, Q., Xie, W., Wan, S., Zhou, Y., & Pei, Q. (2021). Convolutional Neural Networks for forecasting flood process in Internet-of-Things enabled smart city. *Computer Networks*, 186, 107744.

[17] Seydi, S. T., Saeidi, V., Kalantar, B., Ueda, N., van Genderen, J. L., Maskouni, F. H., & Aria, F. A. (2022). Fusion of the multisource datasets for flood extent mapping based on ensemble convolutional neural network (CNN) model. *Journal of sensors, 2022*(1), 2887502.

[18] Kim, K., Kim, J., Choi, H., Kwon, O., Jang, Y., Ryu, S., ... & Cha, S. W. (2023). Pre-diagnosis of flooding and drying in proton exchange membrane fuel cells by bagging ensemble deep learning models using long short-term memory and convolutional neural networks. *Energy*, 266, 126441.

[19] Nkwunonwo, U. C., Whitworth, M., & Baily, B. J. S. A. (2020). A review of the current status of flood modelling for urban flood risk management in the developing countries. *Scientific African*, 7, e00269.

[20] Hu, F., Yang, Q., Yang, J., Luo, Z., Shao, J., & Wang, G. (2024). Incorporating multiple grid-based data in CNN-LSTM hybrid model for daily runoff prediction in the source region of the Yellow River Basin. *Journal of Hydrology: Regional Studies*, 51, 101652.

[21] Zhang, Y., Zhou, Z., Van Griensven Thé, J., Yang, S. X., & Gharabaghi, B. (2023). Flood forecasting using hybrid LSTM and GRU models with lag time preprocessing. *Water,* 15(22), 3982.